Multiparametric imaging of metabolic dysfunction-associated steatotic liver disease using handheld point-of-care ultrasound

Layan Al-Huneidi [1], Leroy Arthur [2], Joshua Hanson [2], Xinlei Gu [3], Xiaoxiao Wang [3], Xiaojing Li [3], Honggui Li [3], Chaodong Wu [3], Kenneth Hoyt [1,2,4]

[1] Department of Electrical and Computer Engineering, Texas A&M University, College Station, TX, USA
[2] Department of Biomedical Engineering, Texas A&M University, College Station, TX, USA
[3] Department of Nutrition, Texas A&M University, College Station, TX, USA
[4] Department of Small Animal Clinical Sciences, Texas A&M University, College Station, TX, USA

***Abstract*—Liver steatosis and inflammation are key features of metabolic dysfunction-associated steatotic liver disease (MASLD) progression. Noninvasive tools capable of distinguishing these phenotypes remain limited. This preclinical study evaluated the use of handheld point-of-care ultrasound (POCUS) imaging and a multiparametric framework for the assessment of MASLD. Both controls and mice with varying degrees of liver steatosis and inflammation were used (4 groups, n = 5 to 7 animals per group). Radiofrequency (RF) data from each animal was acquired using a POCUS system (L20 HD3, Clarius Mobile Health). A multiparametric analysis included the following: attenuation coefficient estimates, US speckle statistics, B-mode echogenicity, and H-mode frequency. After imaging, mice were euthanized and livers excised for quantification of liver steatosis and macrophage infiltration (inflammation). Correlation analysis of multiparametric US and histology results revealed a significant correlation ($R^2 > 0.33$, $p < 0.05$). Support vector machine classification using principal component analysis achieved 95.5% accuracy in MASLD staging. These preclinical results highlight the potential use of a multiparametric POCUS approach for early MASLD detection and staging.**

Keywords—chronic liver disease, multiparametric classification, point-of-care ultrasound.

I. Introduction

Metabolic dysfunction-associated steatotic liver disease (MASLD) is a metabolic condition that spans a spectrum of stages from simple steatosis characterized by fat buildup in the liver to metabolic dysfunction-associated steatohepatitis (MASH) and potentially progressing to fibrosis, cirrhosis, and hepatocellular carcinoma [1]. MASLD is the hepatic component of metabolic dysfunction and is linked to conditions such as hypertension, obesity, type 2 diabetes, insulin resistance, and high cholesterol [2]. In particular, MASH is part of the spectrum of MASLD and is characterized by the development of inflammation as an immune response to fat accumulation and lipotoxicity [3]. The global prevalence of MASLD has increased to about 38% as of 2024 and is particularly prevalent in less developed and remote regions [4]. A meta-analysis on 78 million subjects worldwide found an increase in the prevalence of MASLD in countries with a lower human development index [5]. This prevalence underscores the need for portable and cost-effective diagnostic solutions for the early detection and monitoring of MASLD when the risk of serious complications linked to disease progression is lower.

Noninvasive ultrasound (US) is a commonly used imaging modality for assessing steatosis whereby increased liver echogenicity relative to the kidney serves as a reliable indicator of fat accumulation [6]. Recently, handheld point-of-care US (POCUS) has gained attention as a promising first-line screening tool for MASLD, demonstrating diagnostic accuracy for hepatic steatosis detection that is comparable to traditional cart-based US systems [7]. Quantitative US methods such as B-mode attenuation coefficient [8], [9] or shear wave attenuation coefficient [10] estimation also provide valuable measurements that are closely associated with the progression of liver steatosis. Another category of quantitative US involves analyzing first-order speckle statistics from US envelope data. These methods extract statistical model parameters from US backscattered signals and have been widely applied in the assessment of hepatic steatosis [6]. Multiparametric US approaches that simultaneously incorporate several different US parameters have also been explored for the diagnosis and classification of hepatic steatosis [11], [12]. Nevertheless, studies investigating the use of handheld POCUS devices for the noninvasive assessment of liver inflammation are limited. To that end, this preclinical study evaluated the use of POCUS and multiparametric analysis of mice with varying degrees of MASLD ranging from simple lipid accumulation to inflammation (MASH).

II. Methods

A. Animal models

At 11 to 12 weeks of age, a population of 22 male wild type (WT) C57BL/6J and AlbCre+ mice in which the expression of Cre recombinase is driven by the albumin (Alb) promoter (C57BL/6 background) were obtained from Jackson Laboratory (Bar Harbor, ME). Alb-ADK transgenic (Hep-ADK^{Tg}) mice in which adenosine kinase (ADK) overexpression is driven by the Alb promoter were generated by Cyagen Biosciences Inc (Santa Clara, CA) [13]. Mice were fed a standard chow-diet (CD) and/or fat-enriched methionine and choline-deficient diet (fMCD, 60% fat calories) for 8 weeks (n = 5 to 7 per group). All diets are from Research Diets Inc (New Brunswick, NJ). Study protocols were approved by the Institutional Animal Care and Use Committee of Texas A&M University.

B. Imaging protocol

Mice were anesthetized with 1 to 2% isoflurane in oxygen and placed on a temperature-controlled heating pad to maintain core levels. To ensure optimal US image quality, fur was removed from the abdominal region using electric clippers and then depilatory cream. Coupling gel was then applied and US data was acquired using a portable handheld US system (L20 HD3, Clarius Mobile Health, Vancouver, Canada). This high-frequency 192-element linear array probe has an element pitch of 0.13 mm, center frequency of 14 MHz, bandwidth from 8 to 20 MHz, and data sampling rate of 60 MHz. For each examination, coupling gel was applied and the transducer was placed over the liver region by B-mode US image guidance to ensure maximum visibility and coverage. A single focus was placed distal to target tissue. Autogain was disabled and time-gain compensation (TGC) sliders were fixed ensuring no gain-dependent differences between axial samples. Both B-mode display and RF data were exported for offline analysis.

C. Quantitative US measurements

A rectangular region-of-interest (ROI, depth × width = 5 × 6 mm) was placed over the target liver region. The following image formats were computed from each ROI and represent the multiparametric US approach as detailed in the schematic chart shown in Fig. 1.

C.1. Attenuation coefficient

The US attenuation coefficient α describes the reduction of US amplitude as waves propagate and commonly used to describe liver steatosis [6]. Given a short 32-sample vector of RF data from the liver ROI, the power spectral density was estimated for each column vector using Welch's method. The signal-to-noise ratio (SNR) was then calculated for every column and averaged laterally across the entire ROI [14]. The depth of analysis was shifted by 16 samples and the SNR calculations were performed again until the entire ROI was processed. Linear regression analysis of the SNR versus depth curve for each frequency component was used to obtain the depth-dependent spectral slope. Finally, a linear fit to these spectral slopes across the −6 dB bandwidth was applied to provide a global estimate of the US attenuation coefficient (units dB/cm/MHz). Note this estimation procedure assumes tissue attenuation is constant throughout the entire liver ROI.

C.2. Speckle analysis

Speckle is the grainy pattern seen in US images resulting from the constructive and destructive interference of sound scattered by tissue microstructures. Analyzing statistical properties provides diagnostic information about tissue state. To perform speckle analysis, the envelope of RF data was obtained by applying a Hilbert transform. A root mean square (RMS) normalized histogram was then calculated to derive a probability distribution that was fit to a Nakagami model, and a raw envelope histogram was used to derive a probability distribution that was fit to a Burr model [6]. The Nakagami model describes tissue scattering primarily from point-based or spherical shaped sources. The Burr distribution was introduced to better characterize the US scattering properties of soft vascularized tissues where the dominant scattering sources are cylindrical in shape. Both the Nakagami and Burr distributions are controlled by different shape (m and b) and scale (ω and λ) parameters that are primarily influenced by the range and magnitude of B-mode US image intensities, respectively.

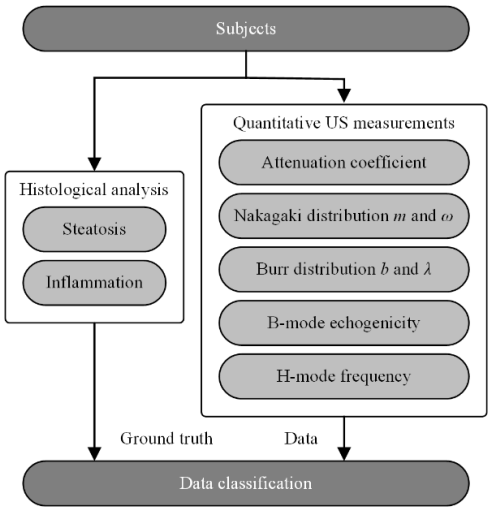

Fig.1. Schematic detailing the quantitative ultrasound (US) analysis of metabolic dysfunction-associated steatotic liver disease (MASLD) using a preclinical mouse model.

C.3. B-mode echogenicity

Brightness-modulated (B-mode) images depict the intensity (echogenicity) of reflected US signals from tissue structures. In MASLD, macrosteatosis is known to increase liver echogenicity [6]. B-mode US image intensity from the liver ROI was calculated as the logarithmic compression of the envelope amplitude after depth-dependent attenuation correction (units dB).

C.4. H-mode frequency

The hue-modulated (H-mode) imaging format uses matched filtering to visualize the relative size and spacing of US scatterers [15]. With increasing liver fat content associated with MASLD progression, it has been shown that H-mode images depict changes in US scatterer size [9]. The H-mode frequency analysis was applied using a Gaussian bandpass filter bank approach [16]. A set of 256 Gaussian functions with a spread of 1 MHz and center frequencies equally spaced across the transducer bandwidth were applied as convolution filters in parallel. The maximum filter output was used to reflect local US scatterer size (units MHz) assuming lower frequency signals are generated from larger scatterers and higher frequency maximum filter outputs from smaller scatterers [17].

D. Multiparametric US analysis

Each spatial US parameter was summarized as a global estimate (i.e., B-mode echogenicity, H-mode frequency, attenuation coefficient α, Nakagami shape m and scale ω, Burr shape b and scale λ) for each animal. Initial correlation analysis revealed high multicollinearity between multiple features so principal component analysis (PCA) was used to reduce dimensionality and remove redundancy. The retained features

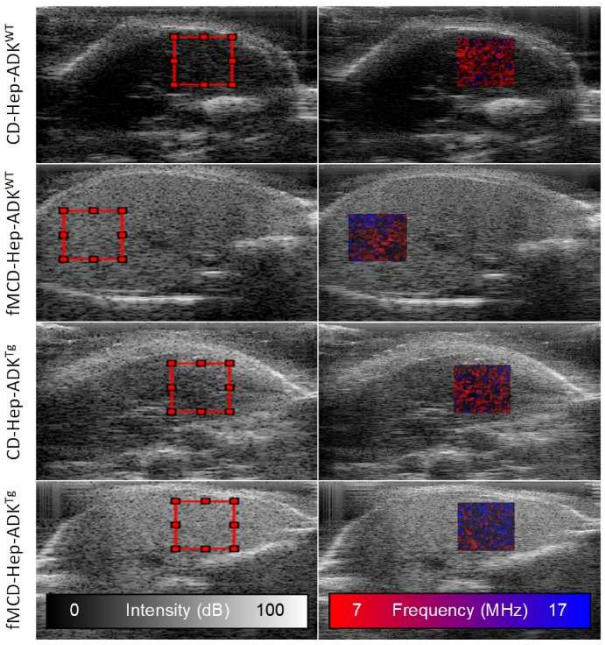

Fig. 2. Representative B-mode echogenicity (left) and F-mode (right) US images and region-of-interest (ROI) selection from four mouse groups, namely, CD-Hep-ADK^{WT}; fMCD-Hep-ADK^{WT}; CD-Hep-ADK^{Tg}; fMCD-Hep-ADK^{Tg}.

were standardized using z-score normalization. A support vector machine (SVM) classifier with a radial basis function (RBF) kernel was used for nonlinear separation of US parameters [11]. Leave-one-out-cross-validation (LOOCV) was used for performance analysis. Hyperparameters including the box constraint and kernel scale parameter gamma were tuned through a grid search across LOOCV folds. After selecting the optimal principal components and SVM configuration, the final model was retrained and evaluated using LOOCV to generate a confusion matrix.

E. Histology

Paraffin-embedded mouse liver blocks were cut into sections of 5 µm thickness and stained with hematoxylin and eosin (H&E) for staging liver steatosis. Specifically, steatosis grading was defined as grades S0 (< 5% steatosis), S1 (5 to 33% steatosis, S2 (34 to 66% steatosis), and S3 (> 66% steatosis) [18]. Additional sections were stained for F4/80 expression with rabbit antibodies (1:100) (AbD Serotec, Raleigh, NC) and analyzed for macrophage infiltration, which was measured as the proportion of macrophages present within a specific area of liver tissue. Note macrophage infiltration is a key marker of liver inflammation associated with MASLD [13].

F. Performance measurements

Nonparametric one-way analysis of variance using the Kruskal-Wallis test corrected for multiple comparisons was used to assess differences between group multiparametric US values. A Pearson correlation analysis assessed linear relationships between each US parameter and steatosis grade or macrophage infiltration. All statistical analyses were done using GraphPad Prism 10 software (San Diego, CA).

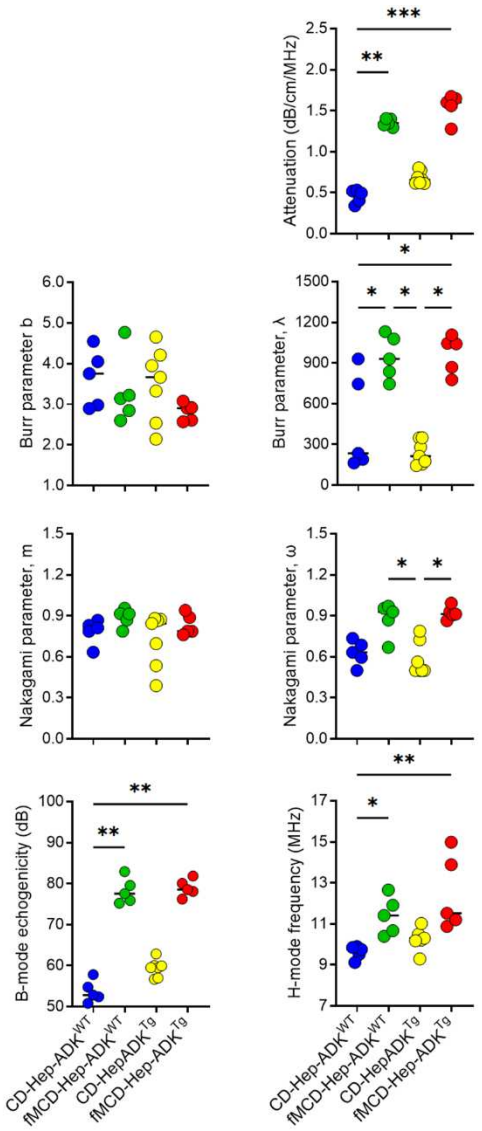

Fig. 3. Summary of multiparametric US measurements from four mouse groups, namely, CD-Hep-ADK^{WT}; fMCD-Hep-ADK^{WT}; CD-Hep-ADK^{Tg}; fMCD-Hep-ADK^{Tg}.

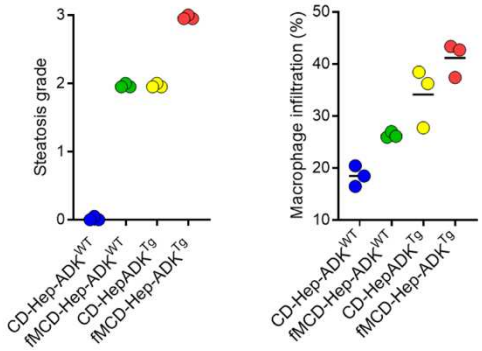

Fig. 4. Histological results and summary of hepatic steatosis (left) and macrophage infiltration (rights) scores.

III. Results and Discussion

Correlation analysis revealed significant associations between steatosis grade and US attenuation coefficient estimates, Burr scale λ, B-mode echogenicity, and H-mode frequency ($R^2 > 0.45, p < 0.02$), which is consistent with previous studies [6]. Regarding liver inflammation, the US attenuation coefficient estimate was the only parameter that correlated with macrophage infiltration ($R^2 = 0.24, p = 0.05$). These findings indicate that steatosis was the dominant driver of quantitative US parameter variation while inflammation appears to influence US attenuation. Representative H-mode frequency overlays depicted in Fig. 2. reveal a progressive blue shift with increasing liver steatosis. Despite having similar steatotic grades, a modest red shift was observed between the fMCD-Hep-ADK^{WT} and CD-Hep-ADK^{Tg} groups suggesting a possible link to inflammatory changes.

As illustrated in Fig. 3, experimental group differences were driven most prominently by US attenuation coefficient estimates, which had the largest separation between groups and captured both amplitude and frequency-dependent changes in tissue properties. Amplitude-related metrics, including Burr scale λ and B-mode echogenicity, were also strong discriminators and contributed more to group separation than the envelope shape and frequency-related parameters. Both Nakagami and Burr shape parameters (m and b) and spectral metrics (H-mode frequency) still played a meaningful role, particularly in the second principal component, suggesting they reflect additional microstructural and spectral differences that complement the amplitude-based measures. A summary of histological results is presented in Fig. 4. These liver tissue measurements highlight the varying steatotic grades and macrophage infiltration levels for each experimental group.

PCA with SVM classification identified two principal components that were able to differentiate cases from the four experimental groups with a prediction accuracy of 95.5%. PCA showed that the US attenuation coefficient, B-mode echogenicity, and Burr scale λ parameter contributed most strongly to the first principal component whereas the Nakagami shape m and Burr shape b parameters contributed to the second principal component, followed by H-mode frequency and Nakagami scale ω. Overall, multiparametric US successfully classified MASLD progression with high accuracy using handheld POCUS.

IV. Conclusion

This research highlights the diagnostic potential of multiparametric US imaging for characterizing MASLD using handheld POCUS and a multiparametric classification model. Preliminary results support the continued development of multiparametric US diagnostic solutions for the accurate detection and monitoring of MASLD, particularly for settings that lack access to more advanced imaging resources.

Acknowledgment

This research was supported in part by National Institutes of Health grants R01CA269973 and R01DK126833.

References

[1] E. C. Z. Lee *et al.*, "The global epidemic of metabolic fatty liver disease," *Curr. Cardiol. Rep.*, vol. 26, no. 4, pp. 199–210, 2024.

[2] H. Zheng, L. A. Sechi, E. P. Navarese, G. Casu, and G. Vidili, "Metabolic dysfunction-associated steatotic liver disease and cardiovascular risk: A comprehensive review," *Cardiovasc. Diabetol.*, vol. 23, no. 1, p. 346, 2024.

[3] M. M. Syed-Abdul, "Lipid metabolism in metabolic-associated steatotic liver disease (MASLD)," *Metabolites*, vol. 14, no. 1, p. 12, 2023.

[4] Z. M. Younossi, M. Kalligeros, and L. Henry, "Epidemiology of metabolic dysfunction-associated steatotic liver disease," *Clin. Mol. Hepatol.*, vol. 31, no. Suppl, pp. S32–S50, 2025.

[5] E. Amini-Salehi *et al.*, "Global prevalence of nonalcoholic fatty liver disease: An updated review meta-analysis comprising a population of 78 million from 38 countries," *Arch. Med. Res.*, vol. 55, no. 6, p. 103043, 2024.

[6] J. Baek, A. El Kaffas, A. Kamaya, K. Hoyt, and K. J. Parker, "Multiparametric quantification and visualization of liver fat using ultrasound," *WFUMB Ultrasound Open*, vol. 2, no. 1, p. 100045, 2024.

[7] O. L. Hernandez, Z. K. S. Yeb, T. Nagi, M. A. Haider, C. Vallejo, and F. Ahson, "Exploring the use of point of care ultrasound in screening for non-alcoholic fatty liver disease: A systematic literature review and meta-analysis," *Arch. Gastroenterol. Res.*, vol. 4, no. 1, Art. no. Issue 1, 2023.

[8] J. Baek *et al.*, "Clusters of ultrasound scattering parameters for the classification of steatotic and normal livers," *Ultrasound Med. Biol.*, vol. 47, no. 10, pp. 3014–3027, 2021.

[9] J. Baek *et al.*, "Multiparametric ultrasound imaging for early-stage steatosis: Comparison with magnetic resonance imaging-based proton density fat fraction," *Med. Phys.*, vol. 51, no. 2, pp. 1313–1325, 2024.

[10] L. Basavarajappa *et al.*, "Multiparametric ultrasound imaging for the assessment of normal versus steatotic livers," *Sci. Rep.*, vol. 11, no. 1, p. 2655, 2021.

[11] J. Baek, L. Basavarajappa, K. Hoyt, and K. J. Parker, "Disease-specific imaging utilizing support vector machine classification of H-scan parameters: Assessment of steatosis in a rat model," *IEEE Trans. Ultrason. Ferroelectr. Freq. Control*, vol. 69, no. 2, pp. 720–731, 2022.

[12] L. Basavarajappa, M. Khairalseed, K. J. Parker, and K. Hoyt, "Development of a multiparametric ultrasound image using an integrated system and method to assess hepatic steatosis," *IEEE South Asian Ultrason. Symp.*, pp. 1–4, 2024.

[13] H. Li *et al.*, "Hepatocyte adenosine kinase promotes excessive fat deposition and liver inflammation," *Gastroenterology*, vol. 164, no. 1, pp. 134–146, 2023.

[14] P. Gong, P. Song, C. Huang, J. Trzasko, and S. Chen, "System-independent ultrasound attenuation coefficient estimation using spectra normalization," *IEEE Trans. Ultrason. Ferroelectr. Freq. Control*, vol. 66, no. 5, pp. 867–875, 2019.

[15] M. Khairalseed and K. Hoyt, "High-resolution ultrasound characterization of local scattering in cancer tissue," *Ultrasound Med. Biol.*, vol. 49, pp. 951–960, 2023.

[16] K. J. Parker and J. Baek, "Fine-tuning the H-scan for discriminating changes in tissue scatterers," *Biomed. Phys. Eng. Express*, vol. 6, no. 4, p. 045012, 2020.

[17] M. Khairalseed, K. Hoyt, J. Ormachea, A. Terrazas, and K. J. Parker, "H-scan sensitivity to scattering size," *J. Med. Imaging*, vol. 4, no. 4, p. 043501, 2017.

[18] N. Azizi *et al.*, "Evaluation of MRI proton density fat fraction in hepatic steatosis: a systematic review and meta-analysis," *Eur. Radiol.*, vol. 35, no. 4, pp. 1794–1807, 2025.